The Tropospheric Lapse Rate and Climatic Sensitivity: Experiments with a Two-Level Atmospheric Model

ISAAC M. HELD[1]

Center for Earth and Planetary Physics, Harvard University, Cambridge, MA 02138

(Manuscript received 31 May 1978, in final form 7 August 1978)

ABSTRACT

The sensitivity of both moist and dry versions of a two-level primitive equation atmospheric model to variations in the solar constant is analyzed. The models have fixed surface albedos, fixed cloudiness and a zero heat flux lower boundary condition, and are forced with annual mean solar fluxes. An attempt is made to understand the response of the static stability in these model atmospheres and the importance of these changes in stability for the climatic responses of other parts of the system.

In the moist model, the static stability increases in low latitudes but decreases in high latitudes as the solar constant increases, resulting in considerable latitudinal structure in the sensitivity of surface temperatures and zonal winds. In the dry model the stability decreases at all latitudes as the solar constant increases. It is argued that this decrease in stability in the dry model, through its effect on isentropic slopes and the supercriticality of the flow, is responsible for the observed large increases in eddy energies and fluxes. Parameterization schemes for the eddy heat flux are critically examined in light of these results.

1. Introduction

In Held and Suarez (1978, hereafter referred to as I) we have described a two-level primitive equation model designed to help gain insights into the gross climatic responses of the atmosphere to perturbations in external parameters. We now analyze this model's sensitivity to the value of the solar constant. We begin in this paper by studying the model's climatic responses when surface albedos are arbitrarily fixed equal to 0.10 everywhere. In a paper to appear shortly (referred to as III) we study the responses when surface albedos are assumed to change with surface temperature so as to crudely take into account the high albedos of ice and snowcover. In both papers, cloud amounts, heights and radiative properties are fixed, and the model is forced with annual mean solar radiation.

The fixed surface albedo experiments described below are of interest first of all because they enable us to better isolate and appreciate the effects of surface albedo-feedback described in III. But they are also of independent interest in that they allow us to study the response of the model dynamics to a relatively simple change in radiative forcing, thus providing tests of some simple theories for the dependence of large-scale eddy fluxes on horizontal and vertical potential temperature gradients. In fact, we shall focus much of our attention on the responses of the model's *vertical* potential temperature gradients to changes in insolation and on the apparently fundamental role played by these changes in determining the model's dynamic responses.

We discuss the sensitivity of two versions of the model—"moist" and "dry"—to perturbations in solar constant. The two versions differ most notably in the manner in which the model atmosphere's static stability is maintained (as described in I). By comparing the responses in moist and dry models, we hope to convince the reader that a precise understanding of the maintenance of the tropospheric lapse rate is crucial for an understanding of climatic sensitivity.

We summarize some of the model results as follows:

- The moist model's static stability decreases in high latitudes but increases in low latitudes as the solar flux increases, the low-latitude response being controlled by the model's moist convective adjustment. As a result of this strong latitudinal dependence in the stability response, the moist model's surface temperatures are twice as sensitive in high as in low latitudes. The strong latitudinal dependence in temperature sensitivity found in the calculations of Wetherald and Manabe (1975) should not, perhaps, be viewed as *entirely* a result of albedo changes in high latitudes (a point also made recently by Ramanathan, 1977).
- The dry model's static stability decreases uniformly at all latitudes as insolation increases. Stone's (1973) theory for such an atmosphere

[1] Present affiliation: Geophysical Fluid Dynamics Laboratory, NOAA, Princeton University, Princeton, NJ 08540.

0022-4928/78/2083-2098$08.00

predicts a slight increase in stability as a result of enhanced vertical sensible heat fluxes by large-scale eddies. A simple calculation similar to Stone's reveals that the discrepancy is primarily due to differences in radiative flux models.

- The most significant response of the moist model's zonal winds to increased solar flux is an increase in the vertical wind shear and the strength of the upper level westerlies in the subtropics. Such a response has been discussed by Kraus (1973) and can be understood as a consequence of the large increase in the static stability of the moist tropical atmosphere. No such response is observed in the dry model.
- As insolation increases we find significant increases in the dry model's eddy kinetic and available potential energies as well as heat and momentum fluxes, but smaller and less uniform changes in the moist model's eddies. The dry results, in particular, cannot be understood using the theories of Green (1970) or Stone (1972), which predict that eddy fluxes are strongly dependent on horizontal temperature gradients but only weakly dependent on static stability. Both theories ignore a crucial parameter through which changes in static stability can have a strong influence on baroclinic eddies, the "supercriticality" of the flow—the ratio of the isentropic slope to the critical slope for baroclinic instability in the quasi-geostrophic two-level model. Following Phillip's original stability analysis, the contention that this critical isentropic slope plays an essential role in extratropical dynamics has been expressed repeatedly. Stone (1978) has recently summarized the observational evidence supporting this contention. That the supercriticality parameter is important for the circulation in a two-level model is certainly not surprising. The question of why eddy fluxes should be strongly dependent on an analogous parameter in continuous atmospheres is addressed in Held (1978). Isentropic slopes increase more or less uniformly at all latitudes with increasing solar flux in the dry experiments, and we attribute to this the larger eddy amplitudes.
- The dry model has a preferred mixing slope for potential temperature equal to roughly half the time-averaged isentropic slope, but this simple result is dependent on the particular diabatic and viscous character of the model flow. In the moist model the mixing slope increases with increasing insolation, larger latent heat release enhancing eddy vertical motions.
- Horizontal energy transport in the moist model increases with increasing insolation primarily because of an increase in the eddy latent heat flux. The Hadley cell's poleward energy transport in the tropics and the eddy dry static energy transport in high latitudes also increase somewhat, but we speculate that these changes are responses to the increased cooling of the subtropics and warming of midlatitudes by the eddy latent heat flux.
- The intensity of moist convection in midlatitudes increases dramatically as the solar flux increases, aided by enhanced low-level moisture convergence in the large-scale eddies. The resulting increase in upper level heating is much larger than any changes in heating due to altered extratropical large-scale energy fluxes. An understanding of the static stability response in midlatitudes requires above all some understanding of this interaction between large-scale eddies and moist convection.

We begin in Section 2 by reviewing the model structure and introducing the sensitivity experiments performed. In Section 3 the responses of the model's zonally averaged temperatures and zonal winds are described, with particular emphasis on the static stability responses. Eddy energies, fluxes, and mixing slopes in the dry model are discussed in Section 4. The moist model's dynamic responses are analyzed in Section 5.

2. The model

As described in I, the two-level primitive equation model utilized for these experiments has variable static stability; potential temperatures as well as horizontal velocities are defined at two levels in the vertical (750 and 250 mb) following Lorenz (1960). The model equations are finite-differenced in the meridional direction (with 3° latitude grid-point spacing) but Fourier decomposed and very severely truncated in the zonal direction. In the experiments described below, only zonal wavenumbers 0, 3 and 6 are retained in the computations; nonlinear interactions with other zonal wavenumbers are ignored. Our motivation for this particular truncation has been discussed in I. Briefly stated, wavenumber 6, typical of strongly unstable waves in midlatitudes, produces a subpolar as well as a subtropical jet in the zonal wind when interacting alone with the zonal flow. A smaller wavenumber, such as 3, capable of efficiently transporting heat into high latitudes, is needed to destroy the polar jet.

Shortwave and longwave radiative fluxes at the top of the atmosphere, at the ground, and at the interface between the two model layers (500 mb) are computed assuming a temperature profile linear in the logarithm of pressure from 1000 to 200 mb, passing through the two predicted temperatures at 750 and 250 mb, and isothermal above 200 mb. The surface is assumed to be flat and to have no heat capacity; surface temperature, sensible heat flux, and evaporation are computed from an energy balance ensuring zero heat flux

through the surface. For the purpose of computing evaporation, the surface is assumed to be saturated. The atmospheric constituents affecting the radiative computations are water vapor, carbon dioxide and clouds. Relative humidity is a fixed function of pressure, independent of latitude, and the CO_2 mixing ratio is fixed independent of latitude and pressure. As stated in the Introduction, cloud amounts, heights and radiative properties are fixed, the surface albedo is fixed at 0.10—a typical albedo in the absence of snow or sea-ice—and the incident flux is given its annual mean values as a function of latitude.

In the moist model, water vapor mixing ratio is a prognostic variable in the lower layer and a moist convective adjustment does not allow the difference in moist static energy between the two model layers to drop below a small positive value determined by a "precipitation criterion" when the lower layer is saturated. In the dry model water vapor is not transported by atmospheric motions and the difference in dry static energy between the two layers is maintained above a small critical value by a dry convective adjustment. Radiative fluxes in the dry model are computed with the same absorber distributions used in the moist model (including fixed relative humidity and cloudiness); the model is, therefore, "dry" only in a very limited sense. Details of the dry and moist convective adjustments, the radiative and surface energy balance calculations, and also the *ad hoc* expressions used for subgrid-scale mixing are given in I.

Calculations are performed with both moist and dry versions of the model at three values of the solar constant—at a standard value of 1360 W m^{-2}, and at solar constants 10% larger and 10% smaller than this standard value. The three experiments with each model allow us to examine the linearity of climatic responses. The large $\pm 10\%$ perturbations have been chosen so that climatic responses can be estimated from integrations of reasonable length. (To the extent that these responses are linear we can, of course, estimate the response to smaller perturbations.) Starting from an isothermal state of rest in each case, we integrate 700 model days and obtain climatic statistics from the final 400 days of each integration. Standard deviations of 400-day time averages are estimated by the procedure outlined in I and are included in several of the figures displaying model results.

We use the notation of I, unless otherwise noted. Subscripts refer to level or to zonal wavenumber, depending on the context. When two subscripts appear on the same symbol, the first refers to the level and the second to zonal wavenumber. The subscripts 1 and 2 refer to the upper and lower levels, respectively. We also use the notation

$$\bar{\rho} \equiv \tfrac{1}{2}(\rho_1+\rho_2) \quad \text{and} \quad \hat{\rho} \equiv \tfrac{1}{2}(\rho_1-\rho_2).$$

Thermal wind balance of the zonal flow is given by

$$-(b/a)(\partial \bar{\Theta}_0/\partial\theta) = f\hat{u}_0$$

in this particular two-level model, where

$$b \equiv -\widehat{(p/p_*)^\kappa} c_p = 0.124 c_p = 124 \text{ m}^2 \text{ s}^{-2} \text{ °C}^{-1}.$$

The mean atmospheric temperature is

$$\bar{T} \equiv \tfrac{1}{2}(T_1+T_2) = \tfrac{1}{2}[(p_1/p_*)^\kappa \Theta_1 + (p_2/p_*)^\kappa \Theta_2]$$
$$= 0.797\bar{\Theta} - 0.124\hat{\Theta}.$$

We occasionally speak of the mean atmospheric temperature gradient as being balanced by coriolis forces, since meridional stability gradients are relatively small:

$$-(b/a)\partial \bar{T}_0/\partial\theta \approx 0.8 f\hat{u}_0.$$

We use braces to denote time averages, and primes, deviations from the time average, i.e., $\rho' \equiv \rho - \{\rho\}$.

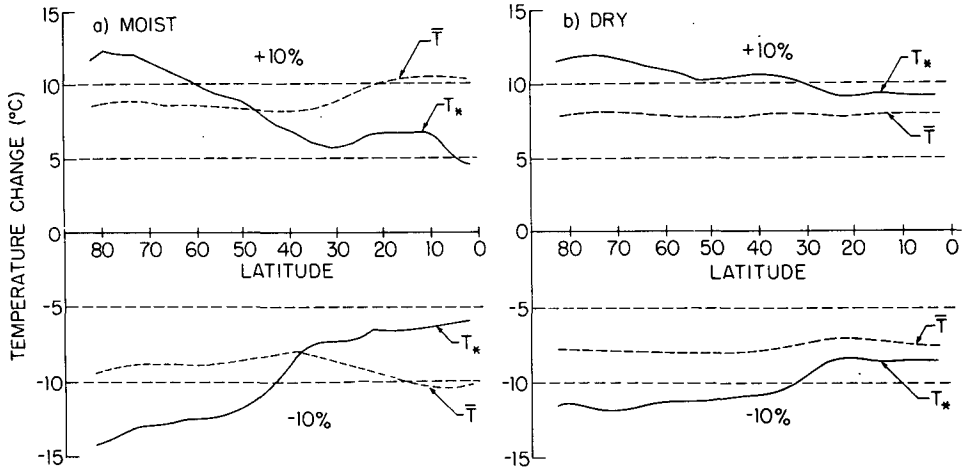

FIG. 1. Temperature changes as a function of latitude when the solar constant is increased and decreased 10% in the (a) moist and (b) dry models. T_* is the surface temperature; $\bar{T}$ the average temperature of the two atmospheric levels.

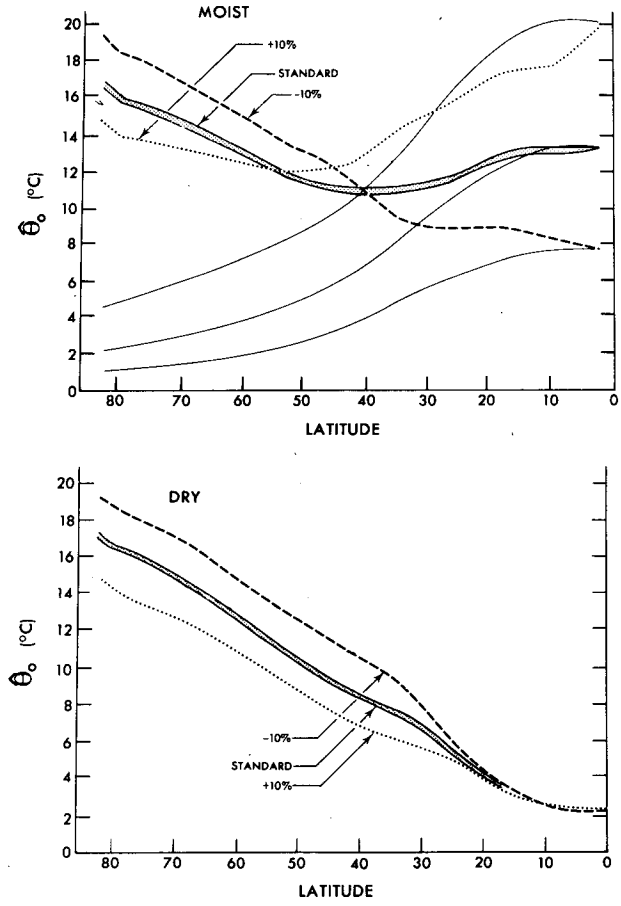

FIG. 2. $\hat{\theta}_0$ at three values of the solar constant in the moist and dry models. Estimated standard deviations of 400-day averages are shown for the standard run. The three solid lines accompanying the moist results are plots of $\hat{\theta}_{\mathrm{CRIT}}(\bar{T})$.

3. The temperature and zonal wind responses

The changes in time-averaged surface temperature T_* and mean atmospheric temperature $\bar{T}$ in the moist model when the solar constant is increased and decreased 10% are shown in Fig. 1a. We note immediately that the sensitivity of the model's surface temperatures is strongly latitude dependent, the response being roughly twice as large in high as in low latitudes. The pole-to-equator surface temperature difference (~37°C in the standard run) decreases more than 2% for each 1% increase in solar flux. The mean atmospheric temperatures react in just the opposite sense, with tropical temperatures somewhat more sensitive than high-latitude mean temperatures. However, the increase in mean tropospheric temperature gradient with increasing insolation is confined to the subtropics (20–35° latitude). If anything, extratropical mean tropospheric temperature gradients decrease slightly with increasing solar flux.

A similar plot of the dry results (Fig. 1b) shows considerably weaker latitudinal dependence in the sensitivity of mean atmospheric temperatures. The significant increase in $\partial\bar{T}/\partial\theta$ with increasing insolation in the subtropics of the moist model is absent in these dry results.

The changes in static stability responsible for these differences in sensitivity are displayed explicitly in Fig. 2. Plotted is the time average of $\hat{\Theta}_0 \equiv \frac{1}{2}(\Theta_{1,0}-\Theta_{2,0})$ for the various experiments. In the moist cases we also plot $\hat{\Theta}_{\mathrm{CRIT}}(\bar{T})$, the stability of the moist adiabat with the same mean atmospheric temperature as that obtained in each moist experiment (see Fig. 3 in I).

In the moist model $\hat{\Theta}_0$ increases sharply in low latitudes and decreases in high latitudes as insolation increases, the increase in low-latitude stability evidently being due to the increasing stability of a moist adiabat with increasing temperature. At the equator, in particular, we have $\hat{\Theta}_0 = \hat{\Theta}_{\mathrm{CRIT}}$. Moist convection occurs continuously in the model's ITCZ, located at the equator, and our moist convective adjustment simply sets $\hat{\Theta} = \hat{\Theta}_{\mathrm{CRIT}}$ when convection is occurring.

We suspect, however, that at least the sign of this response of the low-latitude stability is not sensitive to the particular form of our convective parameterization. The difference in moist static energy between the Hadley cell's poleward flow concentrated near the tropopause and its equatorward flow near the ground is observed to be small (see, e.g., Palmén and Newton, 1969, Chap. 14), but the moist static energy in the poleward flow must be the greater if the cell is to transport energy poleward. An increase in surface temperature is undoubtedly accompanied by a sharp increase in water vapor mixing ratio near the ground. Since the mixing ratio in the poleward flow is negligible, there must be a sharp increase in the difference in dry static energy between the poleward and equatorward flows in order to maintain a poleward energy transport. (In the presence of an ocean, it is not self-evident that the Hadley cell need transport energy poleward, but we are ignoring oceanic heat fluxes here.) If the height of the poleward flow is fixed, as it is in the two-level model, the only option available is for the tropospheric lapse rate to decrease. In reality, the Hadley cell also has the option of increasing its vertical extent, and most likely it will, driven by more intense moist convection; but the large stratospheric static stability maintained by ozone heating prevents any great increase in the height of the poleward flow. The multi-level model of Wetherald and Manabe (1975), in which the Hadley cell does have the option of changing its size, also predicts increasing stability in low latitudes with increasing insolation, as do one-dimensional radiative-convective models which predict the height of the convective heating and the tropospheric lapse rate using more detailed parameterizations of moist convection (Sarachik, 1978).

In midlatitudes of the moist model, the changes in static stability seem a bit more complex. At 45°, $\hat{\Theta}_0$ decreases as the solar flux increases from −10%

to the standard value and then increases as the solar flux is increased an additional 10%. Clearly, the region in which stability is effectively controlled by moist convection spreads poleward as solar insolation increases.

In high latitudes the behavior of the stability is similar in moist and dry models, decreasing with increasing solar flux. The dry model's stability decreases uniformly at all latitudes except near the equator where it is maintained by the dry convective adjustment. We shall argue below that this decrease in stability is of fundamental importance for the response of the dry model's eddy fluxes.

The time-averaged upper and lower level zonal winds in the moist and dry experiments are plotted in Fig. 3. We note the change in strength of the upper level westerlies in the subtropics of the moist model, the accompanying change in vertical shear being geostrophically related to the change in mean atmospheric temperature gradient observed in Fig. 1a. To a first approximation, these responses in the horizontal temperature gradient and vertical shear can be understood as a consequence of the latitudinal dependence in the static stability response and a particular property of the model's radiative fluxes. If we hold the mean atmospheric or 500 mb potential temperature fixed and increase the model's static stability, we find that the infrared flux emitted to space decreases (the parameter b_1 in Table 2 of I is consistently negative). In other words, p_{eff}, the level from which the outgoing flux effectively emanates, is always below 500 mb in our computations, although it is somewhat higher in the tropics than in midlatitudes (Fig. 4). In order to produce the same increase in outgoing flux, the mean atmospheric temperature must increase more in the tropics than in midlatitudes to compensate for the increase in tropical static stability. The changes in outgoing flux as solar insolation increases are not quite latitude independent but these differences turn out to be somewhat smaller than those generated by uncompensated changes in stability.

This response of the subtropical winds is evidently strongly dependent on the details of the radiative flux model. In our radiative calculations we assume, in particular, that cloud amounts and heights are independent of latitude. More high clouds in low latitudes would increase the sensitivity of the outgoing flux to upper level temperatures. This, in turn, could easily push p_{eff} above 500 mb and reverse the sign of the response of the subtropical winds.

This increase in subtropical shears is absent in the dry model, the static stability response being more

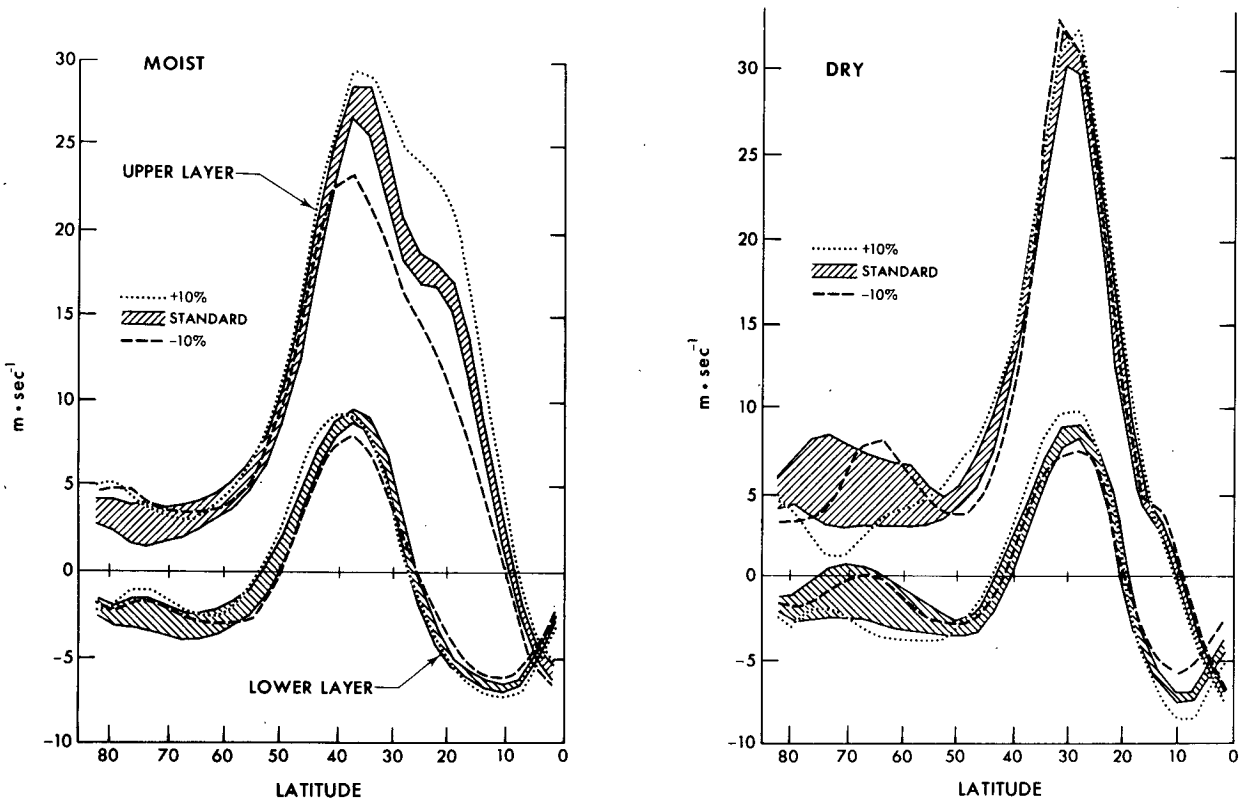

FIG. 3. Upper and lower layer zonal winds at three values of the solar constant in the moist and dry models. Estimated standard deviations of 400-day time averages are shown by the hatched region for the standard run. (Hatched regions in Figs. 5, 6, 8 9, 10, 12 and 13 have the same meaning. See I, Section 4, for a description of the statistical analysis.)

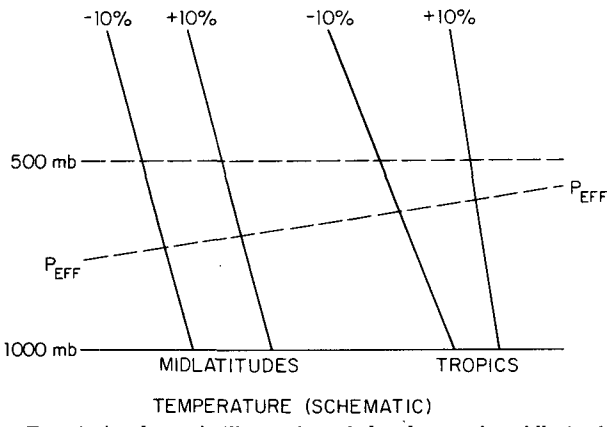

FIG. 4. A schematic illustration of the changes in midlatitude and tropical temperature profiles when the solar constant is changed. If the changes in temperature at $p=p_{\text{eff}}$ are roughly the same at the two latitudes, then 500 mb and mean atmospheric temperatures increase more in the tropics than in midlatitudes, resulting in increased vertical shear in the subtropical winds.

nearly independent of latitude. In fact, the dry model's zonal winds are remarkably insensitive to changes in solar flux. The only significant response we find is a small increase in the strength of the low-level winds in low and middle latitudes with increasing insolation, caused by the larger eddy momentum fluxes described in the following section.

4. Eddy fluxes and energies in the dry model

We have seen that changes in static stability can play an important role in determining the responses of surface temperatures and zonal winds to changes in the solar flux. This static stability response is controlled in part by the large-scale eddy fluxes. These eddy fluxes, in turn, are controlled in part by the static stability response. We approach this complex of problems by first examining the dry model's eddies. The changes in mean temperature gradients are simpler in the dry than in the moist model, and the balance of fluxes maintaining the dry model's static stability is also simpler (see I, Section 7).

Fig. 5 is a plot of the vertically averaged horizontal eddy ($m\neq 0$) and mean ($m=0$) meridional fluxes of potential temperature,

$$\text{Re}\sum_{m=3,6}(v_{1,m}\Theta^*_{1,m}+v_{2,m}\Theta^*_{2,m})$$

and (1)

$$\tfrac{1}{2}(v_{1,0}\Theta_{1,0}+v_{2,0}\Theta_{2,0})=\hat{v}_0\hat{\Theta}_0,$$

for the three dry experiments. The poleward eddy flux increases $\sim 2.5\%$ for each 1% increase in solar flux. There is some compensation due to the increased strength of the Ferrel cell at $\sim 30°$, but this amounts at most to 20% of the increase in the eddy flux. The Coriolis force acting on the meridional circulation in the model's upper layer is closely balanced by eddy momentum fluxes, at least to within 15° of the equator (see Fig. 11 in I); therefore, the increased mean transport in Fig. 5 should be viewed along with the increased eddy heat flux as due simply to larger eddies. In fact, the separation of the total flux into eddy and mean meridional components is rather arbitrary. Denoting the eddy term in (1) as h, and the eddy momentum flux in the upper layer as m, the total flux is

$$h+\hat{v}_0\hat{\Theta}_0\approx-\frac{\hat{\Theta}_0}{f}\left\{-\frac{1}{a\cos(\theta)}\frac{\partial}{\partial\theta}[\cos(\theta)m]-\frac{f}{\hat{\Theta}_0}h\right\},$$

since

$$f\hat{v}_0\approx\frac{1}{a\cos(\theta)}\frac{\partial}{\partial\theta}[\cos(\theta)m].$$

The bracketed expression is the eddy potential vorticity flux in the upper layer of a two-layer quasi-geostrophic system.

Two oft-quoted attempts at developing theories for eddy heat fluxes are those of Green (1970) and Stone (1972). In order to see most clearly that these theories cannot account for the behavior displayed in Fig. 5, we first reduce them to their bare essentials, concentrating on the dependence of the predicted fluxes on vertical and horizontal temperature gradients. We consider only the large Richardson number limit of Stone's expressions.

Stone uses the structure of the most unstable wave in Eady's model to relate eddy meridional velocities and eddy temperatures. The Eady wave's energy is partitioned more or less equally between the kinetic

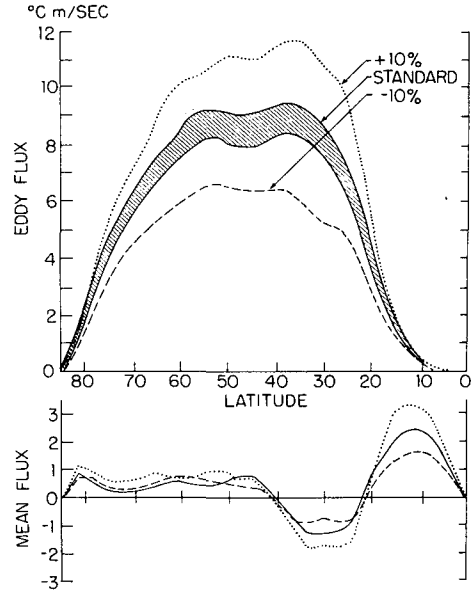

FIG. 5. Vertically averaged horizontal eddy and mean meridional fluxes of potential temperature in the dry model. Estimated standard deviations of 400-day averages are shown for the eddy flux in the standard run.

energy in meridional motions and available potential energy, so such equipartition is also assumed to occur in the statistically steady state of the atmosphere. In our particular two-level model, this implies that

$$\{v'^2\} \propto \{b\Theta'\}^2/(b\hat{\Theta}_0).$$

Assuming that the dependence of the correlation coefficient,

$$\{v'\Theta'\}/(\{v'^2\}\{\Theta'^2\})^{\frac{1}{2}},$$

on the mean temperature gradients is of less importance than that of the variances, we have

$$b\{v'\Theta'\} \propto (b\hat{\Theta}_0)^{\frac{1}{2}}\{v'^2\}.$$

Stone assumes further that eddy kinetic energy is proportional to the baroclinic zonal kinetic energy,

$$\{v'^2\} \propto \hat{u}_0^2 \propto [(b/fa)(\partial\bar{\Theta}_0/\partial\theta)]^2$$

so that

$$b\{v'\Theta'\}_S \propto (b\hat{\Theta}_0)^{\frac{1}{2}}[(b/fa)(\partial\bar{\Theta}_0/\partial\theta)]^2.$$

Green also assumes equipartition between eddy kinetic and eddy available potential energies in those eddies transporting heat, but determines the amplitude of the velocity and temperature perturbations from the assumption that

$$\Theta' \propto \bar{\Theta}_0(20°) - \bar{\Theta}_0(70°) \approx \partial\bar{\Theta}_0/\partial\theta,$$

where 20–70° is taken to be the latitude zone inhabited by strongly unstable eddies. Therefore, Green has

$$\{v'^2\} \propto (b\partial\bar{\Theta}_0/\partial\theta)^2/(b\hat{\Theta}_0),$$

$$b\{v'\Theta'\}_G \propto (b\partial\bar{\Theta}_0/\partial\theta)^2/(b\hat{\Theta}_0)^{\frac{1}{2}}$$

$$\propto b\{v'\Theta'\}_S(a/\lambda_R)^2,$$

where

$$\lambda_R \equiv (b\hat{\Theta}_0)^{\frac{1}{2}}/f$$

is the Rossby radius.

Green's theory might seem the more plausible, since the available potential energy of the basic state is the source of energy for baroclinic instability. But we see that Stone's closure can be obtained from Green's by replacing $\bar{\Theta}_0(20°) - \bar{\Theta}_0(70^0)$ with $(\lambda_R/a) \times (\partial\bar{\Theta}_0/\partial\theta)$. Stone effectively assumes that only the available potential energy within a latitudinal band of width λ_R is actually available to a typical eddy—a plausible assumption if λ_R is its characteristic meridional scale. Pedlosky (1974) makes the same distinction in his criticism of the explanation of Gill *et al.* (1974) for the amplitude of mid-ocean eddies.

Note that $\{v'\Theta'\}_S$ and $\{v'\Theta'\}_G$ have the same quadratic dependence on $\partial\bar{\Theta}_0/\partial\theta$ but $\{v'\Theta'\}_S$ is directly proportional, and $\{v'\Theta'\}_G$ inversely proportional, to $\hat{\Theta}_0^{\frac{1}{2}}$. We note also that $\{v'\Theta'\}_G$ does not depend explicitly on rotation rate, while $\{v'\Theta'\}_S \propto 1/f^2$.

Neither of these theories can account for the behavior of the dry model's eddies. $\partial\bar{\Theta}_0/\partial\theta$ remains essentially unchanged in these experiments, while $\hat{\Theta}_0$ decreases. If we define

$$\langle\hat{\Theta}_0\rangle \equiv \frac{\int \cos(\theta)\hat{\Theta}_0 \,\mathrm{Re}\sum_m \omega_m\bar{\Theta}_m^* d\theta}{\int \cos(\theta)\,\mathrm{Re}\sum_m \omega_m\bar{\Theta}_m^* d\theta},$$

the global mean stability weighted by the eddy kinetic energy generation (a rough guess as to the appropriate

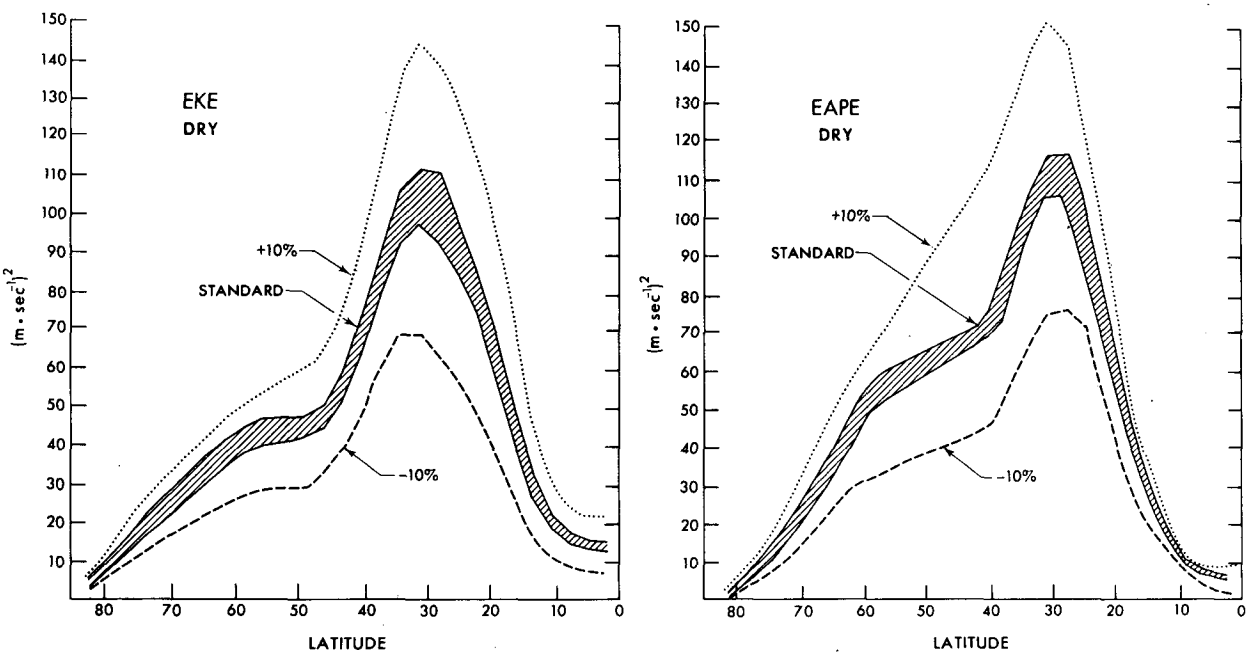

FIG. 6. Eddy kinetic and available potential energy densities in the dry model.

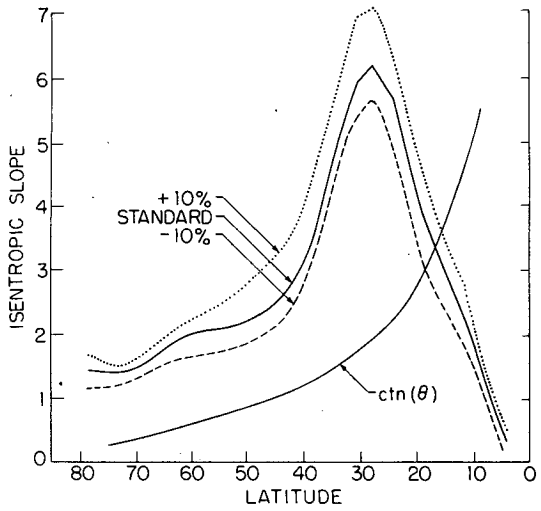

FIG. 7. Latitudinal dependence of the nondimensional isentropic slope $-(\partial\bar{\Theta}_0/\partial\theta)\hat{\Theta}_0^{-1}$ in the dry experiments, compared with the critical isentropic slope ctn(θ).

value of $\hat{\Theta}_0$ for use in testing these theories), we find that

$$\langle\hat{\Theta}_0\rangle^{-\frac{1}{2}}=\begin{cases}(9.25)^{-\frac{1}{2}}=0.33 \text{ for } -10\% \\ (7.71)^{-\frac{1}{2}}=0.36 \text{ for the standard run} \\ (6.47)^{-\frac{1}{2}}=0.39 \text{ for } +10\%\end{cases}$$

or $\sim 0.9\%$ increase for each 1% increase in solar flux. One gets essentially the same result using the values of $\hat{\Theta}_0$ at 30°, near the maximum eddy energy. The $\hat{\Theta}_0^{-\frac{1}{2}}$ dependence of $\{v'\Theta'\}_G$ is too weak to explain the large changes in the model's eddy fluxes.

Equipartition between eddy kinetic and eddy available potential energies, the assumption common to both theories, is rather well obeyed in these dry experiments as shown in Fig. 6. Plotted in the figure are

$$\text{EKE}=\tfrac{1}{2}\sum_{k,m}|\mathbf{v}_{k,m}|^2,$$

$$\text{EAPE}=b\sum_{k,m}|\Theta_{k,m}|^2/2\{\hat{\Theta}_0\}.$$

This rather precise equipartition may be somewhat surprising. Strongly unstable baroclinic waves tend to have their energy equipartitioned, but what relevance does this have for a statistically steady state? Rhines' (1977) study of two-level quasi-geostrophic turbulence suggests that barotropic kinetic energy will accumulate on scales larger than the Rossby radius if the system is sufficiently inviscid and energetic. But our severe spectral truncation confines the eddy ($m=3,6$) energy to scales on the order of λ_R that actively interact with the mean temperature gradient. Furthermore, the model is not particularly inviscid, the dissipative e-folding time for eddy kinetic energy being ~ 3 days. In any case, we learn from Fig. 6, that we are not dealing in these dry experiments with subtle changes in eddy structure. To a first approximation, Green's and Stone's assumptions about eddy *amplitudes*, not their assumptions about *structure*, are violated by the model. Eddy kinetic energy is not proportional to (baroclinic) zonal kinetic energy; neither is it proportional to zonal available potential energy. Zonal kinetic energy does not increase significantly with increasing solar flux, and the slight increase in zonal available potential energy resulting from the decrease in static stability is too small to explain the large increase in heat flux.

Since the decrease in static stability is the only obvious change in the eddy environment as solar flux increases, we suspect that there must be some parameter dependent on static stability which has a strong effect on the eddies. One obvious such parameter is the supercriticality of the flow, the ratio of the vertical shear to the critical shear required for instability in the quasi-geostrophic two-level model on a beta-plane,

$$\hat{u}_c\equiv\beta\lambda_R^2=\beta b\hat{\Theta}_0/f^2.$$

We can also think in terms of a nondimensional critical isentropic slope for instability

$$-\frac{\partial\bar{\Theta}_0/\partial\theta}{\hat{\Theta}_0}\bigg|_c=\frac{f\hat{u}_c}{b\hat{\Theta}_0}=\text{ctn}(\theta).$$

We plot in Fig. 7 the isentropic slopes obtained from the time-averaged potential temperature fields, along with the critical slope ctn(θ). The fractional increase in supercriticality is substantial in midlatitudes, but more modest in the region of maximum eddy energies ($\sim 30°$). Since the model is rather strongly dissipative because of surface drag and radiative damping as well as horizontal diffusion, one might be able to argue that this inviscid criterion overestimates the supercriticality, or average instability of the flow and, therefore, that this average instability varies with solar flux considerably more than is indicated by Fig. 7. In any case, we can think of no more plausible explanation for the large increase in the dry model's eddy heat flux than this increase in supercriticality.

In Fig. 8, we plot the vertical eddy flux of potential temperature across 500 mb,

$$-2\,\text{Re}\sum_m\omega_m\bar{\Theta}_m^*$$

in the three experiments. We estimate $\sim 4\%$ increase for each 1% increase in solar insolation, a substantially larger fractional increase than that observed in the horizontal flux. It is often argued that horizontal and vertical eddy fluxes should satisfy a relation of the form

$$\{\omega'\Theta'\}\{\partial\Theta/\partial p\}\approx-\lambda\{v'\Theta'\}\{\partial\Theta/\partial y\}, \qquad (2)$$

where λ, a constant, is thought of as the slope of the surface along which potential temperature is mixed, divided by the slope of the isentropic surface. For example, Stone (1972) chooses $\lambda=0.42$, the ratio

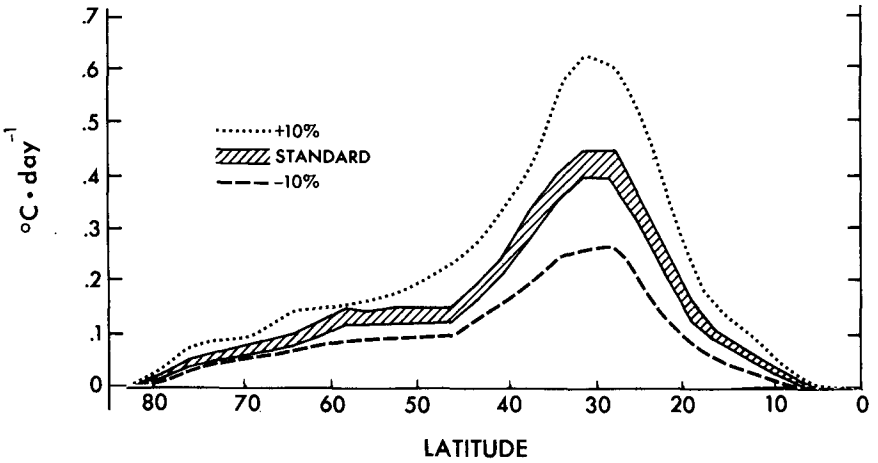

FIG. 8. Vertical eddy flux of potential temperature across 500 mb $-2\,\mathrm{Re}\sum_m \omega_m \bar{\Theta}^*_m$, where ω_m is the eddy vertical p velocity divided by $\Delta p \equiv 500$ mb, so that the vertical flux has the units of a heating rate.

produced by the most unstable wave in Eady's model halfway between the upper and lower boundaries. Such a relation would explain the large increase in vertical flux as due partly to the smaller increase in horizontal flux and partly to the decrease in static stability.

The significance of this sort of mixing argument for the model's statistically steady state can best be understood by examining the balance of terms maintaining the eddy potential temperature variance, a balance involving generation by the downgradient horizontal flux H, destruction by the upgradient vertical flux $-V$, destruction by radiative damping and diffusion $-R-D$, and possible generation or destruction by the convective adjustment P (and in the moist model by latent heat release). In the steady state

$$0=\left\langle \frac{\partial}{\partial t}\{\tfrac{1}{2}\sum_{k,m}|\Theta_{k,m}|^2\}\right\rangle$$

$$=\langle H\rangle+\langle V\rangle+\langle R\rangle+\langle D\rangle+\langle P\rangle,$$

where the angle brackets denote a global average, and where

$$H\equiv-\left\{\sum_{k,m}\mathrm{Re}(v_{k,m}\Theta^*_{k,m})\frac{1}{a}\partial\Theta_{k,0}/\partial\theta\right\},$$

$$V\equiv-\{2\,\mathrm{Re}\sum_m(\omega_m\bar{\Theta}^*_m)\hat{\Theta}_0\},$$

$$R\equiv-\{\sum_{k,m}|\Theta_{k,m}|^2/\tau_{\mathrm{RAD}}\},$$

$$D\equiv-\left\{\frac{D}{a^2}\sum_{k,m}\left(\left|\frac{\partial\Theta_{k,m}}{\partial\theta}\right|^2+\frac{m^2}{\cos^2(\theta)}|\Theta_{k,m}|^2\right)\right\},$$

$P\equiv\{$GENERATION DUE TO PRECIPITATION AND CONVECTION$\}$.

Following the notation used in I, Eq. (1), ω is here the vertical p velocity divided by $\Delta p=500$ mb. We list the values of the various terms in Table 1 for each of the experiments, both moist and dry. (The moist cases are included for later comparison.) The ratio between the loss due to vertical fluxes and the generation by horizontal fluxes is analogous to the constant λ in (2), so we denote $-\langle V\rangle/\langle H\rangle$ by λ^*. (Time correlation coefficients between the zonally averaged eddy horizontal flux and horizontal temperature gradient are observed to be small (~-0.15), and correlations between eddy vertical flux and static stability are even smaller—so we need not distinguish, for example, between $\{\mathrm{Re}(v_{k,m}\Theta^*_{k,m})\partial\Theta_{k,0}/\partial\theta\}$ and $\{\mathrm{Re}(v_{k,m}\Theta^*_{k,m})\}\{\partial\Theta_{k,0}/\partial\theta\}$.) We find that λ^* is very nearly equal to 0.55 in each of the dry experiments. The constancy of this ratio is impressive, considering the substantial changes in horizontal flux, vertical flux, and static stability.

The fact that λ^* is roughly 0.5 is not unrelated to the equipartition between EKE and EAPE noted above. If eddy kinetic energy and temperature variance have roughly the same dissipative time scale, τ, then

$$\partial\langle\mathrm{EKE}\rangle/\partial t\approx-b\langle V\rangle/\langle\hat{\Theta}\rangle-\langle\mathrm{EKE}\rangle/\tau,$$

$$\partial\langle\mathrm{EAPE}\rangle/\partial t\approx b(\langle H\rangle+\langle V\rangle)/\langle\hat{\Theta}\rangle-\langle\mathrm{EAPE}\rangle/\tau,$$

TABLE 1. The balance of terms maintaining the eddy potential temperature variance and the ratio of the destruction through upgradient vertical transport to the generation through down-gradient horizontal transport λ^*. See text for definitions of the symbols used.

	Dry			Moist		
	−10%	0%	+10%	−10%	0%	+10%
H	1.71	2.25	2.78	1.52	1.75	2.14
V	−0.75	−1.24	−1.52	−1.16	−1.57	−2.05
R	−0.25	−0.33	−0.38	−0.25	−0.27	−0.34
D	−0.48	−0.63	−0.76	−0.61	−0.66	−0.80
P	−0.03	−0.06	−0.12	0.50	0.75	1.05
$\lambda^*\equiv\lvert V\rvert/H$	0.56	0.55	0.55	0.76	0.90	0.96

ignoring the small conversion of EKE to zonal kinetic energy. In the statistically steady state,

$$\langle \mathrm{EKE}\rangle/\langle \mathrm{EAPE}\rangle \approx -\langle V\rangle/(\langle H\rangle+\langle V\rangle),$$

so that if

$$\langle V\rangle/\langle H\rangle \approx -\tfrac{1}{2},$$

then

$$\langle \mathrm{EKE}\rangle/\langle \mathrm{EAPE}\rangle \approx 1.$$

In our experiments about 70% of the loss of both EKE and EAPE is due to lateral diffusion and, in fact, EKE and EAPE do have roughly the same dissipative e-folding times. But this result evidently depends on the character of the model's dissipation. In reality, temperature variance and kinetic energy may very well be lost through quite different processes. An example of a two-level model calculation in which the effective e-folding time for temperature variance is much longer than that for eddy kinetic energy is that of Barros and Wiin-Nielsen (1974). From their Fig. 2 we estimate $\lambda^* \approx 0.93$. In the Simmons and Hoskins (1978) study of the life cycle of a baroclinic wave, they find $\lambda^* \approx 0.5$ during the exponentially growing phase of the wave, but $\lambda^* \approx 1$ averaged over the life cycle (see their Fig. 5). Substantial kinetic energy is lost to dissipation in the frontal zones of their mature disturbance, but little temperature variance is lost.

It seems clear, on the one hand, that the concept of mixing slope fixed in its relation to the isentropic slope is valuable in interpreting the large changes in vertical fluxes in Fig. 8, and, on the other hand, that this relation is determined in part by our subgrid-scale mixing. One cannot rule out the possibility that the viscous or diabatic character of the flow will itself change substantially when the system is perturbed, so that the relation between mixing and isentropic slopes will not be fixed. A good example of just this sort of behavior is provided by the moist model as described in Section 5.

We can now summarize this discussion of the dry results with a simple calculation which incorporates our understanding of the interrelationships between fluxes and mean gradients and predicts the observed climatic responses. The calculation is patterned after that in Stone (1973). It can be thought of as applying to some domain average of these variables or, perhaps, to their values near 30°, where the vertical flux and eddy energies have their maxima and where the convergence of the horizontal flux is small. For clarity, we denote the vertically averaged horizontal potential temperature flux by h and the vertical flux across 500 mb by v.

The relation between mixing slope and isentropic slope discussed above,

$$v \propto h\hat{\Theta}^{-1}(\partial\bar{\Theta}/\partial y),$$

yields for small perturbations,

$$\delta \ln v \approx \delta \ln h + \delta \ln \partial\bar{\Theta}/\partial y - \delta \ln \hat{\Theta}. \tag{3a}$$

Choosing Stone's expression for the horizontal flux, but adding some unspecified dependence on isentropic slope, we have

$$\begin{aligned} h &\propto \hat{\Theta}^{\frac{1}{2}}(\partial\bar{\Theta}/\partial y)^2 F(I); \qquad I \equiv \hat{\Theta}^{-1}(\partial\bar{\Theta}/\partial y), \\ \delta \ln h &\approx (\tfrac{1}{2}-G)\delta \ln\hat{\Theta} + (2+G)\delta \ln(\partial\bar{\Theta}/\partial y), \end{aligned} \tag{3b}$$

where

$$G \equiv \partial \ln F/\partial \ln I.$$

Two relations for the effects of the fluxes on the mean gradients are needed to close this set of equations.

The convergence of the horizontal flux is balanced by radiative heating or cooling. If we ignore the small difference between eddy potential temperature and energy fluxes, then

$$\partial h/\partial y \approx \mathcal{L}_1(y) - Qs(y)$$

where $\mathcal{L}_1$ is the infrared flux emitted to space, Q the solar constant, and $s(y)$ the latitudinal distribution of the absorbed solar flux. Differentiating with respect to y, and using the result that the changes in the meridional structure of h are negligible, so that $\partial^2 h/\partial y^2 \propto -h$, we obtain

$$h \propto (Q\partial s/\partial y - \partial \mathcal{L}_1/\partial y).$$

The dependence of $\mathcal{L}_1$ on $\bar{\Theta}$ and $\hat{\Theta}$ can be found in Table 2 in I. Since $\partial\hat{\Theta}/\partial y$ does not vary significantly in the dry experiments, we find $\partial\mathcal{L}_1/\partial y \approx \gamma\partial\bar{\Theta}/\partial y$ with $\gamma \sim 2.2$ W m^{-2} °C and nearly independent of temperature over the relevant temperature range. Therefore,

$$h \propto (\partial\bar{\Theta}_E/\partial y - \partial\bar{\Theta}/\partial y),$$

where

$$\partial\bar{\Theta}_E/\partial y \equiv \gamma^{-1}Q\partial s/\partial y.$$

Defining

$$\alpha \equiv \frac{\partial\bar{\Theta}_E/\partial y}{\partial\bar{\Theta}_E/\partial y - \partial\bar{\Theta}/\partial y}$$

and perturbing Q, the result is

$$\delta \ln h \approx \alpha\delta \ln Q - (\alpha-1)\delta \ln(\partial\bar{\Theta}/\partial y). \tag{3c}$$

From Fig. 9 in I we estimate $\alpha \approx 2$.

The final equation, relating vertical flux and stability, is most easily obtained from the potential temperature balance in the model's upper layer. Averaged over the domain, or at a latitude where the horizontal convergence is zero, the vertical flux must balance the radiative cooling of the upper layer, $v \propto \mathcal{L}_1 - \mathcal{L}_2$, where $\mathcal{L}_2$ is the net infrared flux at 500 mb (positive upward). We ignore the small changes in fractional solar absorption with changing temperature. Using Table 2 in I once again, linearizing about the values of $\bar{\Theta}_0$, $\hat{\Theta}_0$, $\mathcal{L}_1$ and $\mathcal{L}_2$ at 30° in the standard experiment for definiteness and setting $\delta \ln\mathcal{L}_1 \approx \delta \ln Q$,

we find that

$$\delta \ln v \approx 4.4\delta \ln Q + 0.6\delta \ln \hat{\Theta}. \tag{3d}$$

Eqs. (3a) and (3c) yield $\delta \ln v \approx 2\delta \ln Q - \delta \ln \hat{\Theta}$, after setting $\alpha = 2$. Using (3d) we obtain

$$\frac{\delta \ln \hat{\Theta}}{\delta \ln Q} \approx -1.5, \qquad \frac{\delta \ln v}{\delta \ln Q} \approx 3.5,$$

more or less as observed in the dry calculations.

The decrease in $\hat{\Theta}$ with increasing solar flux is evidently another result dependent on a particular feature of the radiative flux model. This decrease depends on the coefficient of $\delta \ln Q$ in (3d) being greater than 2. It is this feature of our radiative model that results in the discrepancy between our static stability response and that predicted by Stone (1973). The large value of this coefficient results from our upper level longwave cooling being small $[(\mathcal{L}_1 - \mathcal{L}_2)/\mathcal{L}_1 \approx 0.15]$ and increasing rapidly with increasing temperature, the rapid increase, in turn, being a consequence of the assumption of fixed relative humidity. A truly dry, CO_2 atmosphere, for example, very well might have a different static stability response and, therefore, a very different dynamic response to variations in solar heating.

In the absence of any dynamic response in Eq. (3d), the radiatively induced fractional change in stability is exceptionally large, $\delta \ln \hat{\Theta}/\delta \ln Q \approx -7$. This illustrates a simple but very important point. When there is no dynamic response, temperatures and temperature gradients undergo small changes in response to a radiative perturbation. But if the static stability is small, as it is in these dry experiments, the fractional change in vertical *potential* temperature gradient can be relatively large. If horizontal and vertical potential temperature gradients are equally important for the dynamics (as they are if isentropic slopes are important), then the static stability balance will likely be the key to the dynamic response.

Eqs. (3a) and (3b) now determine $\delta \ln h/\delta \ln Q$ and $\delta \ln(\partial\bar{\Theta}/\partial y)/\delta \ln Q$ as functions of G, and we can determine G from the observed responses. $G \approx 2$ results in $\delta \ln h/\delta \ln Q \approx 2$ and $\delta \ln(\partial\bar{\Theta}/\partial y)/\delta \ln Q \approx 0$ in rough agreement with Figs. 1 and 5. If, for the sake of argument, we modify Stone's theory by assuming that the eddy kinetic energy in those eddies transporting heat is proportional, not to the available potential energy within a latitudinal span of width λ_R, $\propto (\partial\bar{\Theta}/\partial y)^2$, but only to the supercritical part of this available potential energy, i.e., proportional to

$$\left[\left(\frac{\partial\bar{\Theta}}{\partial y}\right)^2 - \left(\frac{\partial\bar{\Theta}}{\partial y}\bigg|_c\right)^2\right],$$

then

$$F(I) \equiv 1 - \left(\frac{I_c}{I}\right)^2 \quad \text{and} \quad G(I) \equiv \frac{2}{(I/I_c)^2 - 1},$$

where I_c is the critical isentropic slope. If $G \approx 2$, then $I/I_c \approx 2^{\frac{1}{2}}$, not an entirely unreasonable value of the supercriticality, glancing back at Fig. 7 and recalling that the inviscid stability criterion may not be quite appropriate for our rather viscous flow.

5. The moist eddy energies and fluxes

The behavior of the moist eddies is more complex than that of their dry counterparts. This is immediately apparent from Table 1, which shows that the mixing slope for potential temperature, normalized by the isentropic slope, increases with increasing insolation in the moist experiments. Indeed, this normalized

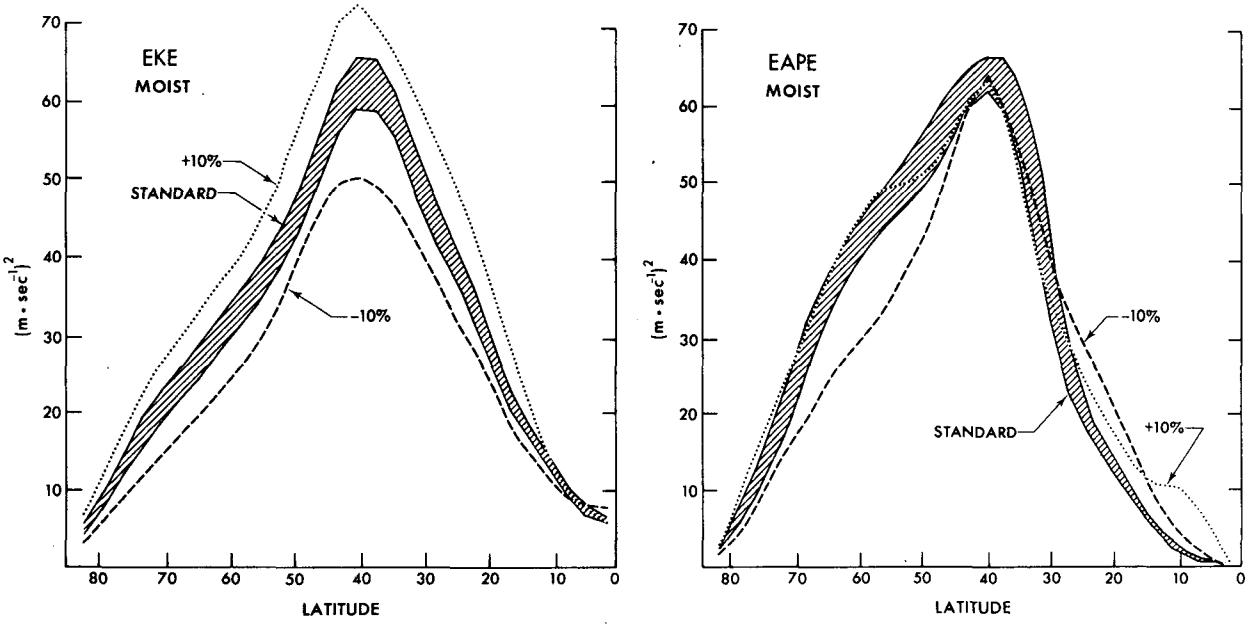

FIG. 9. Eddy kinetic and available potential energy densities in the moist model.

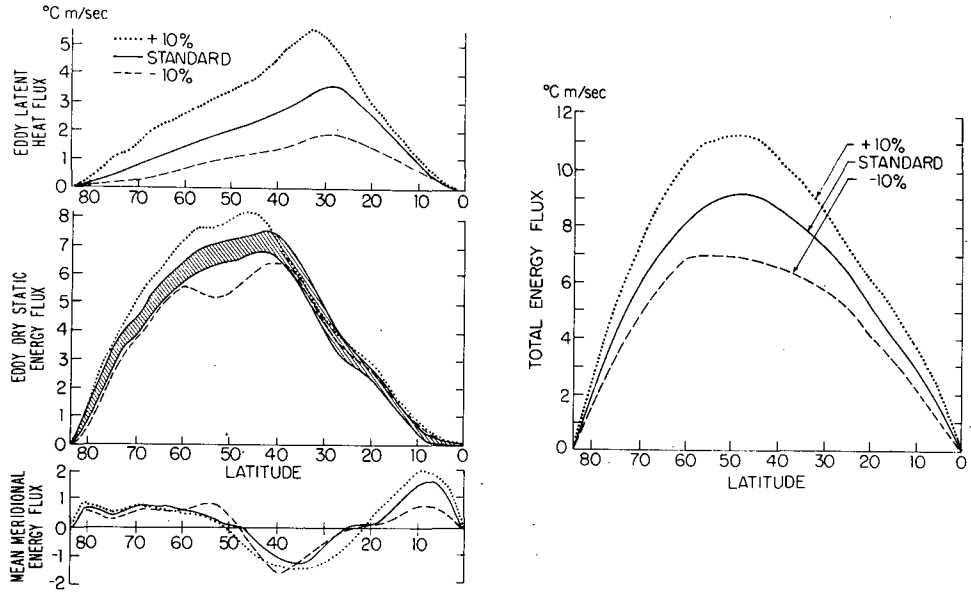

FIG. 10. Various contributions to the vertically averaged meridional flux of energy, as well as the total flux of moist static energy, in the moist model. (The flux of kinetic energy is negligible.)

mixing slope is much larger in the three moist cases than in any of the dry experiments. Table 1 also indicates that latent heating, being correlated with temperature, is a significant source of temperature variance (i.e., P is large). It is this latent heating that enhances vertical velocities and steepens trajectories. [Manabe and Smagorinsky (1967, Fig. 4.6) obtain very similar results in their comparison of moist and dry multi-level GCM's.] Thus, unlike their dry counterparts, moist eddies respond to changes in solar flux with significant changes in structure as well as amplitude.

Eddy kinetic and available potential energies are plotted in Fig. 9 for the three moist experiments. The kinetic energies increase uniformly with increasing insolation, but the complicated behavior of the eddy available potential energy suggests that the increase in EKE does not have a simple explanation. The transition from -10% to the standard case in high latitudes is qualitatively similar to that in the dry experiments, in that EKE and EAPE both increase. Elsewhere the increase in EKE seems to be due to increased generation resulting from steeper trajectories.

We divide the poleward flux of moist static energy into 1) the eddy flux of dry static energy, 2) the eddy flux of latent heat and 3) the mean meridional flux of moist static energy:

$$1)\quad \mathrm{Re}\sum_m [v^*_{1,m}(\bar{T}_m+A\hat{\Theta}_m)+v^*_{2,m}(\bar{T}_m-A\hat{\Theta}_m)]$$

$$2)\quad \mathrm{Re}L/c_p\sum_m v^*_{2,m}r_m$$

$$3)\quad \tfrac{1}{2}[v_{1,0}(\bar{T}_0+A\hat{\Theta}_0)+v_{2,0}(\bar{T}_0-A\hat{\Theta}_0+Lr_0/c_p)]$$
$$=\hat{v}_0(A\hat{\Theta}_0-Lr_0/2c_p).$$

[Multiply by c_p to obtain energy fluxes; $A=0.797$]. The various contributions and the total flux in the three experiments are displayed in Fig. 10. The rapid increase in eddy latent heat flux with increasing insolation is the dominant response. The eddy dry static energy flux increases only in high latitudes and rather modestly, while the mean meridional flux increases significantly only in the deep tropics. The net result of these varied responses is a more or less uniform increase in the total poleward energy flux of $\sim 2.5\%$ for each 1% increase in solar constant. This result is very different from that of Wetherald and Manabe (1975), who find that their latent heat flux increases while their dry static energy flux decreases with increasing insolation, producing almost no change in the total flux. As we shall describe in III, our model's climatic responses resemble more closely those of Wetherald and Manabe when a small polar icecap and surface albedo feedback are introduced into the calculations.

The increase in the eddy latent heat flux, arising simply from the greater vapor content of the air, results in enhanced midlatitude heating, since this flux peaks at 30°. We suspect that the increase in eddy sensible heat flux from middle to high latitudes can be thought of as the response of the high latitude eddies to this increase in midlatitude heating. A similar explanation can be given for the changes in mean meridional transport. We have argued in I that the model Hadley cell's energy transport near the equator is determined by the energy transport out of the tropics and by the requirement of small tropical temperature gradients. If this argument is correct, then the increase in the mean meridional flux in the deep tropics in these experiments is primarily a re-

sponse to the increased cooling of the subtropics by the poleward eddy latent heat flux.

Perhaps it is worth emphasizing that the total poleward energy transport is very poorly described by a constant diffusivity, and even more poorly described by a diffusivity proportional to the meridional temperature gradient. Fig. 11a is a plot of the diffusion constant D_E obtained by dividing the eddy transport of dry static energy by the mean atmospheric temperature gradient,

$$a^{-1}D_E\partial\bar{T}_0/\partial\theta \equiv \mathrm{Re}\sum_m [v^*_{1,m}(\bar{T}_m+A\hat{\Theta}_m)+v^*_{2,m}(\bar{T}_m-A\hat{\Theta}_m)]. \quad (4)$$

Not only do we see the effect of increased transport in high latitudes unaccompanied by an increase in meridional temperature gradient, but also the effect of increased meridional temperature gradients in the subtropics unaccompanied by an increase in transport. (Similar results are obtained if one divides the eddy potential temperature flux by the mean potential temperature gradient.) Fig. 11b is a plot of the effective diffusivity for the total meridional transport of energy D_T obtained by substituting the total transport for the eddy transport in (4). D_T increases by a factor of 2 near 50°, much of the increase being due to latent heat transport. We also calculate D_* such that $D_*\partial T_*/\partial\theta = D_T\partial\bar{T}_0/\partial\theta$, where T_* is the surface temperature. D_* is the sort of diffusivity required by models which attempt to express meridional energy transports in terms of local surface temperature gradients. Changes in D_* (Fig. 11c) are even larger than those in D_T—surface temperature gradients decrease substantially (Fig. 1) and energy transports increase substantially as solar flux increases.

Since surface temperatures play no direct dynamic role in the present model—they are computed only

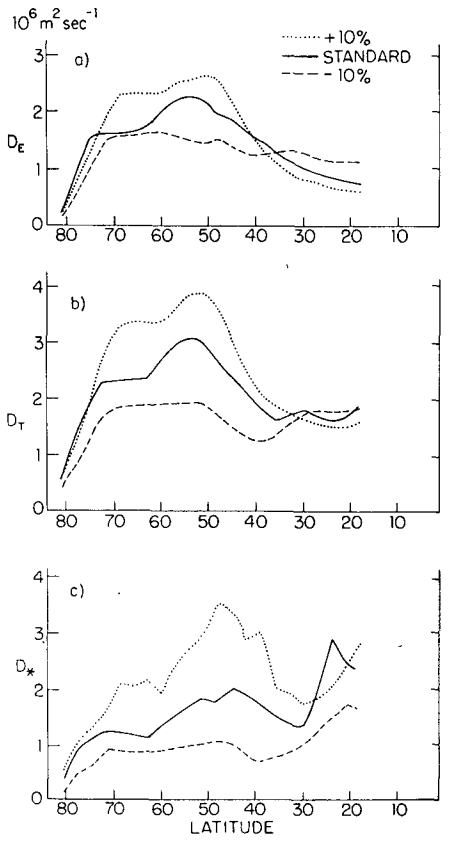

FIG. 11. Effective diffusion constants in the moist experiments for computing (a) eddy transport of dry static energy using mean atmospheric temperature gradients (D_E), (b) total energy transport using mean atmospheric temperature gradients (D_T), and (c) total energy transport using surface temperature gradients (D_*). Effective diffusivities equatorward of 20° are not shown; they are highly variable because of the small tropical temperature gradients.

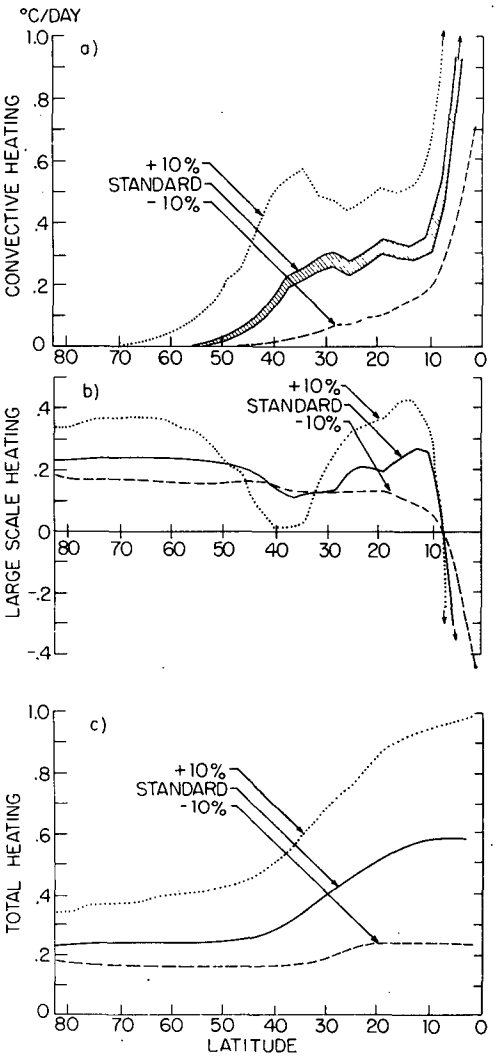

FIG. 12. Heating rate in the upper layer of the moist model due to (a) moist convection, (b) large-scale (resolved) dynamics and (c) the sum of (a) and (b), which must equal the radiative cooling.

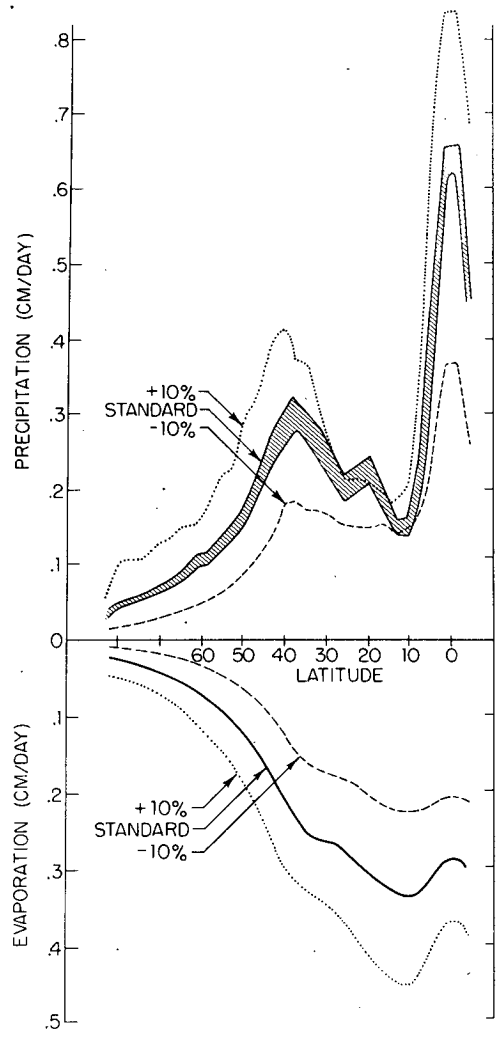

FIG. 13. Evaporation and precipitation in the moist model. Estimated standard deviations of 400-day averages are shown for precipitation in the standard run. Variability in evaporation is negligible in comparison.

for the purpose of balancing radiative and surface fluxes—criticism of surface temperature-based diffusive energy balance models on the basis of Fig. 11c is somewhat unfair. Surface or near-surface temperature gradients may in fact play an important dynamic role, as suggested by the Charney-Stern necessary condition for baroclinic instability. If this is the case, this role will certainly be distorted by the two-level model.

Turning to the vertical energy fluxes, additional complications are introduced by moist convection. In fact, changes in the moist convective fluxes overwhelm changes in large-scale vertical fluxes and clearly determine the static stability response in midlatitudes.

In Fig. 12 we plot the heating of the model's upper layer due to moist convection in the three experiments, along with the total dynamical heating or cooling due to large-scale motions resolved by the model. We also plot the sum of the large-scale and small-scale heating. As discussed in I, we can control the strength of the rising motion in the model's ITCZ with our "precipitation criterion" without changing the radiation deficit, so the division of the nonradiative heating at the equator into large- and small-scale components is certainly dependent on the convective parameterization. Therefore, focusing on the midlatitudes we see that changes in upper level convective heating are several times larger than changes in large-scale dynamic heating. In the +10% experiment, moist convection invades the region of maximum baroclinic activity and low-level moisture convergence in the eddies produces a midlatitude maximum in convective heating. Evidently, one cannot understand upper level midlatitude convective heating and, therefore, the midlatitude static stability, without some understanding of this generation of convection by baroclinic eddies.

Some compensation between large- and small-scale heating is apparent in Fig. 12. Large-scale heating decreases in the +10% experiment at the latitude of the largest increase in convective heating, resulting in a radiation deficit in the upper layer that is a smooth function of latitude. The vertical large-scale energy flux has not disappeared; rather, the convergence of the eddy horizontal flux and the Ferrel cell have shifted slightly so as to cancel the convergence of the vertical flux in the upper layer. It seems unlikely that these subtle changes in large-scale dynamic heating can be understood in isolation, without simultaneously understanding the moist convective heating. The moist eddies must be considered as entities which respond to mean temperature and humidity fields, and which produce smooth changes in these mean fields.

Since much of the interest in climatic sensitivity studies focuses on the hydrologic cycle, we present the model's precipitation and evaporation patterns in Fig. 13. The globally averaged strength of the hydrologic cycle increases ~3.5% for each 1% increase in the solar constant. Precipitation increases everywhere except in the subtropics. Unlike the energy balance, where large mean meridional fluxes of dry static energy and latent heat of opposite sign nearly balance in low latitudes, thereby increasing the relative importance of the eddy fluxes, the low-latitude moisture balance is dominated by the mean meridional flux. This equatorward flux increases with increasing insolation and is able to maintain constant precipitation in the subtropics in the face of greatly enhanced evaporation. While the total energy transport by the Hadley cell is insensitive to our convective parameterization (see Fig. 21 in I), the equatorward moisture transport is not (Fig. 19 in I); so we do not take these interesting changes in the low-latitude hydrologic cycle too seriously.

The 3.5% increase in evaporation is due partly to

the rapid increase in downward longwave flux with increasing temperature and vapor concentrations in the lower atmosphere, and partly to a decrease in Bowen's ratio, as discussed by Wetherald and Manabe (1975). Some details can be found in Held (1976).

We attempt no simple synthesis of these moist results similar to that presented for the dry cases in Section 4. In the dry calculations, changes in horizontal and vertical temperature gradients are relatively uniform with latitude; we could, in analyzing these calculations, avoid addressing problems arising from the substantial meridional extent of the midlatitude eddies and the resulting nonlocal character of the eddy fluxes. In the moist calculations, changes in these gradients are of opposite sign at different latitudes, and we cannot ignore these problems. Changes in eddy structure, particularly changes in the preferred slope along which potential temperature is mixed by the large-scale motions, are another complicating factor. Most importantly, the amount of upper level heating due to moist convection in midlatitudes is evidently related to the large-scale eddy amplitudes. The response of the midlatitude static stability in a moist atmosphere to perturbations in external parameters promises to be a particularly challenging problem in climate theory.

6. Concluding remarks

Many parts of the climatic system which are certainly of great importance for the climatic response to variations in the solar flux have been ignored in these calculations. The reader can undoubtedly provide a list. Yet a host of problems still arise when one tries to understand responses in this severely restricted system, even when one eliminates the complexities due to moist convection and moisture transport. We have tried to focus on some of these problems, particularly those involving the static stability response. This response is important in both moist and dry models but for different reasons.

Because the contribution of moist convection to the stability balance varies with latitude, the static stability in the moist model responds differently at high and low latitudes to perturbations in the solar flux. The result is significant latitudinal structure in the sensitivity of surface temperatures and well as mean atmospheric temperatures and zonal winds, structure not present in the dry model. These changes in stability are large. Whereas in our standard experiment static stability is nearly independent of latitude, in the -10% experiment it varies by a factor of 2 from pole to equator. *Unless we are being misled by this model, the observed uniformity of the tropospheric lapse rate with latitude is simply a coincidence.* These large changes in stability presumably have an effect on the moist eddies, but as outlined in Section 5, the latitudinal nonuniformity and the dependence of the moist eddies on the moisture as well as temperature field makes it difficult to isolate this effect.

The effects of stability variations in the dry model are more easily discerned. We argue that these variations in stability exert their influence on the large-scale eddies primarily by altering the ratio of the isentropic slope to the critical slope required for instability. Our model is too severely truncated and too viscous to allow us to make any quantitative statements about this influence, but it seems clear that supercriticality can play an important, if not dominant, role in determining climatic responses in *two-level models*. The question of the relevance of these results immediately arises, since the simplest zonal flows in continuously stratified atmospheres require no critical isentropic slope for instability (Charney, 1947). There is, however, an analogous parameter in the continuous case, the ratio of the height $h \equiv f^2(\partial\bar{u}/\partial z)/(\beta N^2)$ to the scale height H of the atmosphere, i.e.,

$$\frac{h}{H} = -\frac{a\partial\Theta/\partial y}{H\partial\Theta/\partial z}\tan(\theta).$$

Unless this parameter exerts analogous control over the eddy dynamics in continuous atmospheres, the two-level model will be of little value for climatic studies. We have argued in Held (1978) that the eddy heat flux does, in fact, fall rapidly to very small values when h/H drops substantially below unity. But this argument is based on a scaling analysis whose validity has not been demonstrated. A satisfying theory for the poleward heat flux in the atmosphere does not exist.

Acknowledgments. This work is part of a collaborative study with Max J. Suarez. Some of the ideas presented here are very likely Max's. We both thank S. Manabe for his helpful advice and comments. Conversations with R. Lindzen and E. Sarachik helped clarify the analysis of the numerical results. Support was provided by NOAA Grant 04-3-00233 and National Science Foundation Grant GA-40341 through the GFD Program at Princeton University, and by NSF Contract ATM-20156 at Harvard.

REFERENCES

Barros, V. R., and A. Wiin-Nielsen, 1974: On quasi-geostrophic turbulence: A numerical experiment. *J. Atmos. Sci.*, **31**, 609–621.

Charney, J. G., 1947: The dynamics of long waves in a baroclinic westerly current. *J. Meteor.*, **4**, 135–162.

Gill, A. E., J. S. A. Green, and A. Simmons, 1974: Energy partition in the large-scale ocean circulation and the production of mid-ocean eddies. *Deep-Sea Res.*, **21**, 499–528.

Green, J. S. A., 1970: Transfer properties of large scale eddies and the general circulation of the atmosphere. *Quart. J. Roy. Meteor. Soc.*, **96**, 157–185.

Held, I. M., 1976: The tropospheric lapse rate and climatic sensitivity. Ph.D. thesis, Princeton University, 217 pp.

——, 1978: The vertical scale of an unstable baroclinic wave and its importance for eddy heat flux parameterizations. *J. Atmos. Sci.*, **35**, 572–576.

——, and M. J. Suarez, 1978: A two-level primitive equation atmospheric model designed for climatic sensitivity experiments. *J. Atmos. Sci.*, **35**, 206–229.

Kraus, E. B., 1973: Comparison between ice age and present general circulations. *Nature*, **245**, 129–133.

Lorenz, E. N., 1960: Energy and numerical weather prediction. *Tellus*, **12**, 364–373.

Manabe, S., and J. Smagorinsky, 1967: Simulated climatology of a general circulation model with a hydrologic cycle. II. Analysis of the tropical atmosphere. *Mon. Wea. Rev.*, **93**, 155–169.

Palmén, E., and C. W. Newton, 1969: *Atmospheric Circulation Systems*. Academic Press, 603 pp.

Pedlosky, J., 1974: A note on the amplitude of baroclinic waves in the mid-ocean. *Deep-Sea Res.*, **22**, 575–576.

Ramanathan, V., 1977: Interaction between ice-albedo, lapse rate, and cloud-top feedbacks: An analysis of the nonlinear response of a GCM climate model. *J. Atmos. Sci.*, **34**, 1885–1897.

Rhines, P., 1977: The dynamics of unsteady currents. *The Sea: Ideas and Observations on Progress in the Study of the Seas*, E. D. Goldberg, Ed., Wiley (see pp. 189–318).

Sarachik, E. S., 1978: Tropical sea surface temperature: An interactive one dimensional atmosphere-ocean model. *Dyn. Atmos. Oceans*. (in press).

Simmons, A. J., and B. J. Hoskins, 1978: The life cycles of some nonlinear baroclinic waves. *J. Atmos. Sci.*, **35**, 414–432.

Stone, P. H., 1972: A simplified radiative-dynamical model for the static stability of rotating atmospheres. *J. Atmos. Sci.*, **29**, 405–418.

——, 1973: Effects of large-scale eddies on climate change. *J. Atmos. Sci.*, **30**, 521–529.

——, 1978: Baroclinic adjustment. *J. Atmos. Sci.*, **35**, 561–571.

Wetherald, R. T., and S. Manabe, 1975: The effects of changing the solar constant on the climate of a general circulation model. *J. Atmos. Sci.*, **32**, 2044–2059.